Project No. 13-5332

Development of Novel Porous Sorbents for Extraction of Uranium from Seawater

Fuel Cycle Research and Development

Wenbin Lin
University of Chicago

Stephen Kung, Federal POC
Phil Britt, Technical POC

Development of Novel Porous Sorbents for Extraction of Uranium from Seawater

Wenbin Lin – The University of Chicago

Project 13-5332

Final Report

Background and Significance

Climate disruption is one of the greatest crises the global community faces in the 21st century. Alarming increases in CO_2, NO, SO_2 and particulate matter levels will have catastrophic consequences on the environment, food supplies, and human health if no action is taken to lessen their worldwide prevalence.

Nuclear energy remains the only mature technology capable of continuous base-load power generation with ultralow carbon dioxide, nitric oxide, and sulfur dioxide emissions. Over the lifetime of the technology, nuclear energy outputs less than 1.5% the carbon dioxide emissions per gigawatt hour relative to coal—about as much as onshore wind power.[1] However, in order for nuclear energy to be considered a viable option in the future, a stable supply of uranium must be secured.

Current estimates suggest there is less than 100 years' worth of uranium left in terrestrial ores (6.3 million tons) if current consumption levels remain unchanged.[2] It is likely, however, that demand for nuclear fuel will rise as a direct consequence of the ratification of global climate accords. The oceans, containing approximately 4.5 billion tons of uranium (U) at a uniform concentration of ~3 ppb, represent a virtually limitless supply of this resource.[3] Development of technologies to recover uranium from seawater would greatly improve the U resource availability, providing a U price ceiling for the current generation and sustaining the nuclear fuel supply for future generations.

Several methods have been previously evaluated for uranium sequestration including solvent extraction, ion exchange, flotation, biomass collection, and adsorption; however, none have been found to be suitable for reasons including cost effectiveness, long term stability, and selectivity.[4,5] While polymer beads and fibers have been functionalized with amidoxime functional groups to afford U adsorption capacities as high as 1.5 g U/kg,[6] further discoveries are needed to make uranium extraction from seawater economically feasible.

R&D Progress / Status

EXAFS Analysis of Polymer Fibers

Despite nearly thirty-five years of active research,[7] there is no consensus as to the precise coordination environment of uranyl bound to amidoxime-functionalized polymer fiber. To be sure, there has been crystallographic evidence of a monodentate amidoxime binding motif,[3] a tridentate motif,[8] an η^2 motif,[9] and a chelating amidoxime motif[10] with a molybdenum center (Figure 1). However, there have not been any reports of rigorous charaterization of the uranium binding environement on state-of-the-art polymer fibers. Since the absence of long-range ordering precludes crystallographic study, we have used x-ray absorption fine structure (XAFS) spectroscopy and extended x-ray absorption fine structure (EXAFS) analysis in order to investigate the uranyl coordination environment as bound by polyamidoxime fibers.

Six samples were prepared for analysis—four polymer fibers and two small molecule standards. Of the polymer fibers, one was contacted with seawater for 56 days at Pacific Northwest National Laboratory and used as received; one was contacted with seawater for 56 days and eluted of all metals except uranium and vanadium; one was contacted with seawater simulant containing uranyl nitrate for 24 hours; and one was contacted with seawater simulant containing uranyl nitrate and sodium orthovanadate for 24 hours. The small molecular standards—uranyl glutarimidedioxime and uranyl benzamidoxime exhibited the tridentate motif and η^2 amidoxime binding motifs respectively. All samples were studied at beamline 10BM-B[11] of the Advanced Photon Source at Argonne National Laboratory.

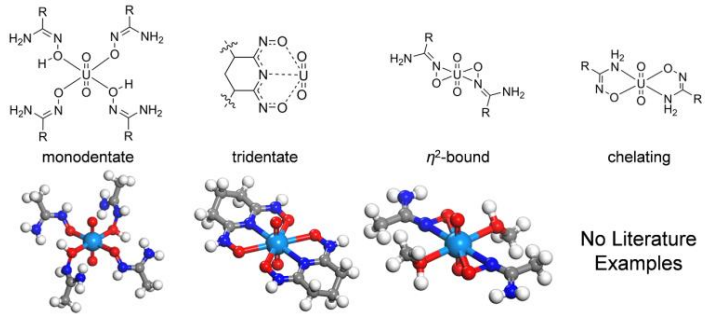

Figure 1: Crystal structures corresponding to proposed coordination motifs for how amidoxime binds the uranyl cation.

Direct comparison of the R-space EXAFS spectra reveals distinct differences among the samples (Figure 2). Specifically, the small molecule standard with the tridentate-binding mode possesses a peak at approximately 2.2 Å which is not present in any of the other spectra, as well as a broad peak at 3 Å. Deconvolution of the calculated scattering paths responsible for these features reveal they can be assigned to direct scattering off the imine nitrogen (2.2 Å) and the combination of direct scattering from oxime N and C as well as multiple scattering from the axial O on uranyl.

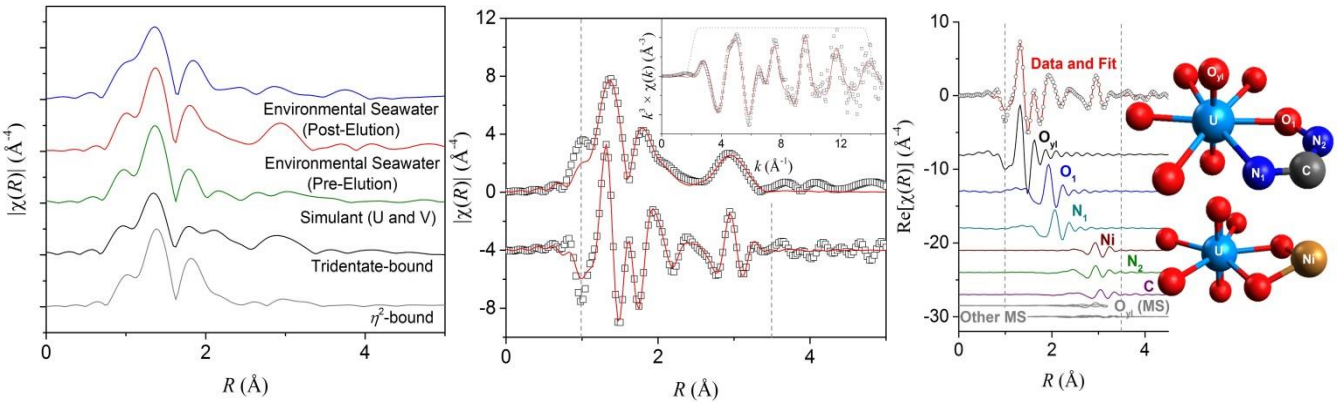

Figure 2: (Left) EXAFS spectra for small molecule standards and amidoxime-functionalized polymer fibers collected at the uranium L_{III} edge. (Center) Data (squares) and fit (red line) of the polymer fibers exposed to seawater simulant containing uranium and vanadium. The lower plot is the real-space component of the Fourier transform, while the upper plot is the magnitude of the Fourier transform. (Right) Data (red line) and fit (open circles) for the real component of the Fourier transform of seawater-contacted polymer fibers, with direct scattering paths from the structure model offset underneath.

The best fit model of the simulant-contacted fibers consists of 5.6 ± 1.2 (U only) or 6.2 ± 1.4 (U and V) light scattering elements, while the third shell contains 2.8 ± 1.2 of both N and C (U only) or 3.4 ± 1.1 of both N and C (U and V). This model is consistent with 2-3 amidoximes binding in a chelating fashion or two chelating amidoximes and one monodentate-bound ligand.

The first and second shells of the EXAFS spectra for the environmental seawater-contacted polymer fibers are fit in a manner identical to the previous samples. The first shell consists of the O_{yl} scattering paths, while 2.8 ± 0.6 oxygen and an equivalent number of nitrogen comprise the second shell. However, a large scattering contribution at 3 Å in R-space, similar to the spectrum of the tridentate-binding cyclic imide dioxime, cannot be readily fit with a chelating model. No such feature was observed in the simulant-contacted fibers.

Based on reported single crystal data, it has been hypothesized that a Ni scatterer is the contributor in the 3 Å region due to having an appropriate U-Ni bond length around 3.5 Å. However, a comparison of EXAFS spectra collected at the Ni K-edge reveals a distinct lack of any features around 3 Å in R-space (Figure 3). Therefore, it is unlikely that the feature observed around 3 Å in the seawater contacted fibers is due to bound Ni in the second coordination sphere. The precise identity of the species responsible for the large feature is still under investigation.

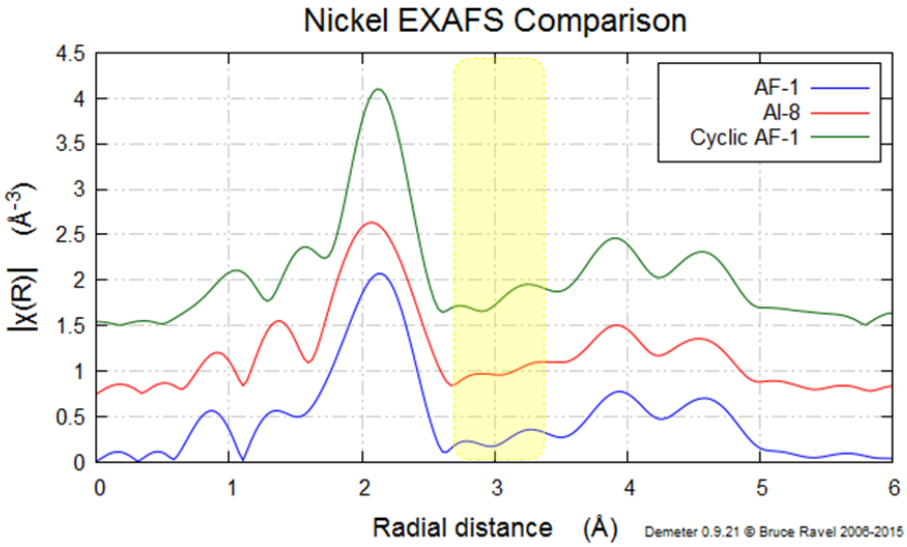

Figure 3 Nickel EXAFS of seawater contacted polymer fibers of AF-1 formulation, AI-8 formulation, and Cylic AF-1 formulation

The implications of these findings are significant and challenge several long-held assumptions. The EXAFS fits reveal multiple amidoxime functionalities must bind one uranyl, invalidating the paradigm of single-ligand binding and requiring updated models for the analysis of these complex systems. Cooperative binding requires at least two functionalities to interact with uranyl, suggesting polymer conformation may influence sorption capacity more significantly than previously considered. This research was recently accepted for publication in *Energy and Environmental Science.*[12]

Studies on Emergent Behavior

Interested by the cooperative binding effect observed in the seawater contacted fibers above, further studies were conducted to elucidate the fundamental nature of the observed phenomenon. A series of polymer adsorbents prepared by radiation induced graft polymerization (RIGP) were contacted with aqueous UO_2^{2+} and investigated by XAFS to determine the U binding environment.[13]

In contrast to results from crystallographic, computational, and *in situ* XAFS investigations using small molecule analogs, amidoxime displays a distinctly different binding mode when incorporated into a polymer and is thus an example of an emergent phenomenon which can only be induced when included as part of a larger system. Although seeming to possess spectral features indicative of tridentate binding, fitting the XAFS spectrum for a brine-contacted AI-8 adsorbent revealed including the cyclic imide dioxime binding site resulted in a fit which was less statistically rigorous than fits performed without the cyclic binding site (Figure 4).

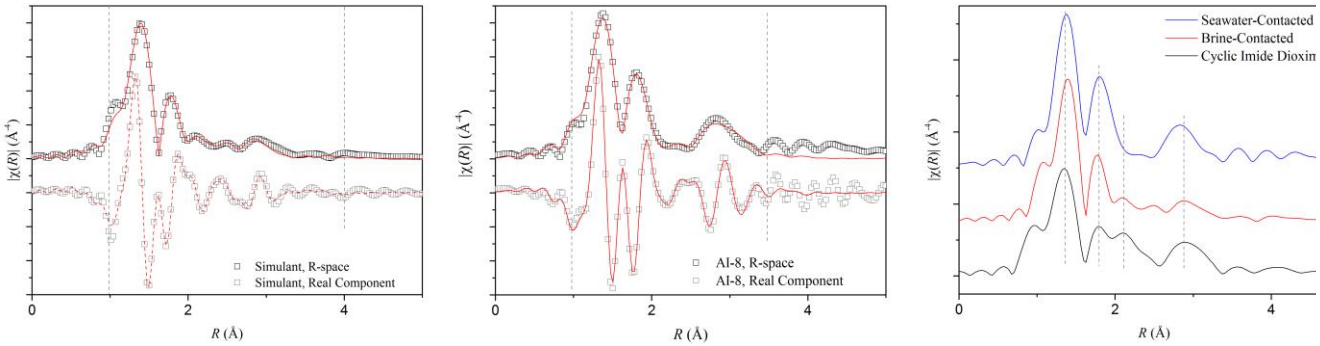

Figure 4. Data (squares) and fit (line) of AI-8 exposed to brine (left) and environmental seawater (center). The lower plot is the real-space component of the Fourier transform, while the upper plot is the magnitude of the Fourier transform. The grey dashed lines represent the region over which the data were fitted. Fit of EXAFS spectra for Brine-contacted AI-8. (Center) Fit of EXAFS spectra for seawater-contacted AI-8. (Right) Comparison of brine- and seawater-contacted AI-8 with the cyclic imide dioxime small molecule standard.

The seawater-contacted AI-8 displayed a large feature at 3Å, similar to a related adsorbent investigated previously, but in contrast to earlier results, the persistence of the peak following treatment with dilute HCl suggests that the transition metal is strongly bound by the fiber, with Fe proposed as the oxo-bridged species. Beyond simply identifying the uranium binding environments on these adsorbents, these results provide an important example of emergent behavior and constitute a critical starting point for subsequent studies in this developing field of research. Emergent phenomena have been reported in a wide number of systems, but amidoxime adsorbents constitute the first instance where the metal binding environment is directly affected by integration within a polymer. Due to the tunability of the polymer formulation, these materials are amenable to further investigation regarding the onset and persistence of emergent behavior,

and are expected to afford critical knowledge for the rational design of advanced materials with enhanced performance for selective metal ion separations.

Bifunctional Chelator for Ultrahigh Uranium Uptake

Intrigued by the cooperative binding effect observed in the polymer fiber samples, we endeavored to design, synthesize, and characterize a bifunctional chelating ligand for ultrahigh uptake of uranium. Density functional theory calculations were used to quickly and efficiently screen several bifunctional ligand derivatives for favorable uranyl binding prior to the commencement of synthesis. All structures were based on the diaryl ether framework due to the inherent flexibility of the –COC– linkage and the ease with which sites adjacent to the oxygen could be functionalized. The diaryl ether can be functionalized either *ortho* or *meta* to the bridging oxygen and both options were investigated computationally (Figure 5).

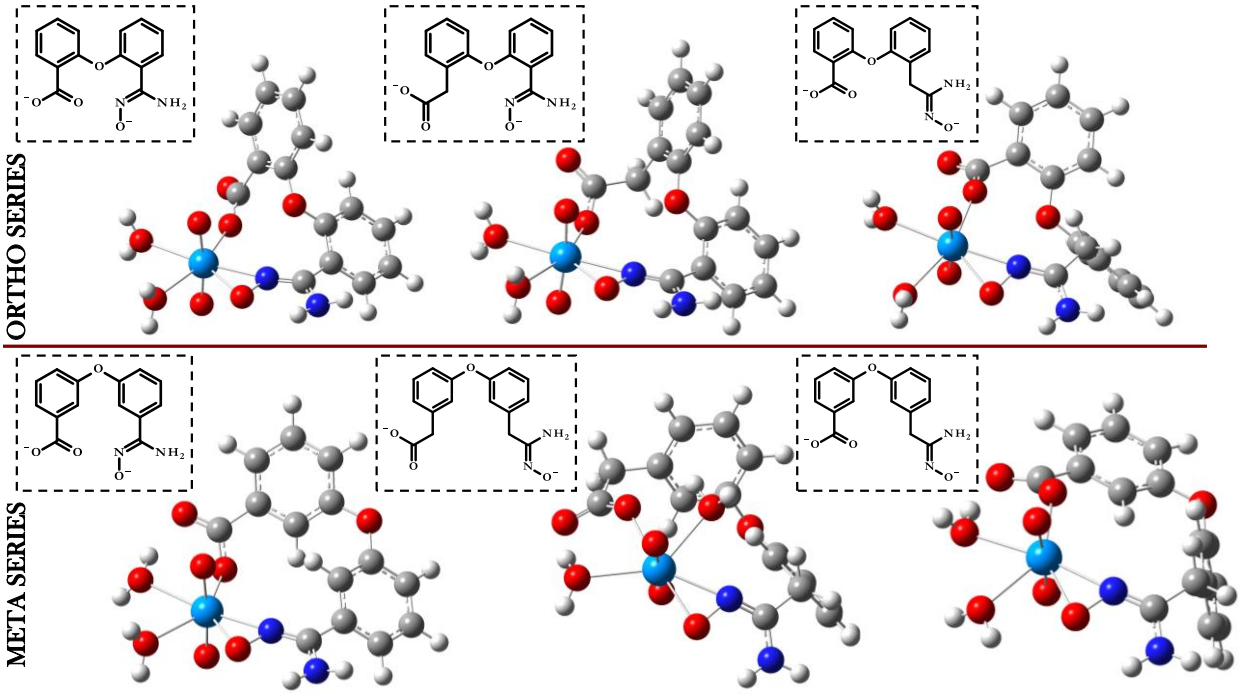

Figure 5: DFT optimized structures of chelator-bound UO_2^{2+}. Functionalization at the ortho position is displayed in the top panel, while the analogous meta-functionalized ligand is displayed in the bottom panel. Red, white, gray, dark blue, and light blue spheres represent O, H, C, N, and U, respectively. Insets display the chemical structure of the unbound bifunctional chelating ligands.

Sorption studies of the ligand for uranium uptake were conducted in seawater simulant at a pH of 8.2 by agitation on a plate shaker for 18 hours. An exceptional uranium uptake of 553 mg U g^{-1} of sorbent was obtained with a theoretical saturation capacity of 710 mg U g^{-1} obtained by fitting the isotherm data with the Langmuir-Freundlich model (Figure 6). In all cases, addition of chelator to uranyl solutions resulted in instantaneous formation of an amorphous yellow precipitate, regardless of efforts to retard the rate of complexation. As crystallographic study was

not feasible, XAFS analysis was applied to examine the uranium coordination environment after extraction from seawater simulant.

The best fit model is consistent with empirical observations and suggests that strong binding via an η^2 motif is not occurring. The proposed monodentate binding motif conflicts with earlier DFT work, which indicates the η^2 motif is thermodynamically preferred. Thus, the yellow precipitate observed is likely due to the formation of a coordination polymer. Indeed, the rapid uranium adsorption displayed by the bifunctional chelator precludes the formation of the slower, more thermodynamically stable η^2 binding motif suggested by DFT calculations.

This work was recently published in *Industrial and Engineering Chemistry Research* as part of the Uranium from Seawater special issue.[14]

Figure 6: Adsorption isotherm at room temperature. Data points are black squares, with the fit displayed as a red line, R^2 = 98.2%. Inset: the linearized data and fit at dilute uranium concentration.

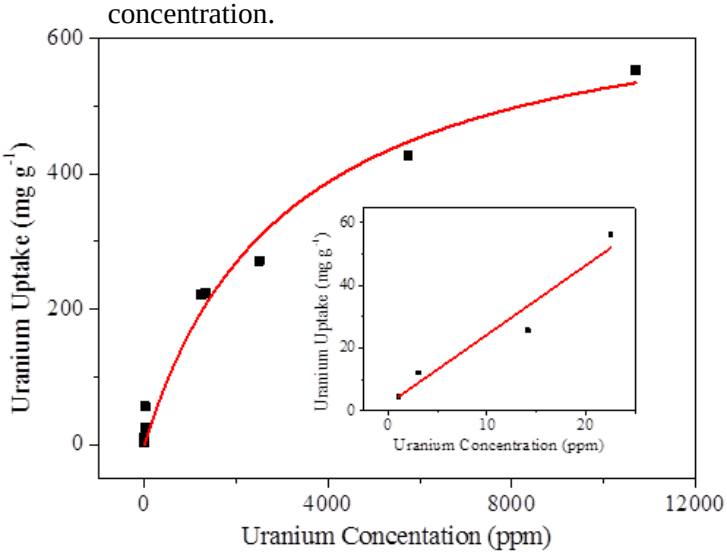

Advanced nanomaterials

Very recent work endeavors to build on the momentum of the previous studies by translating the fundamental knowledge gleaned into advanced, porous nanomaterials. Several batches of hydrogel materials incorporating bifunctional chelating ligands with hydrophilic crosslinkers have recently been synthesized and tested for uranium uptake.

Ligands with ditopic carboxylate or amidoxime functionalies were chosen in order to maximize uranium affinity due to the potential for cooperativity of their functional groups. The bis-amidoxime functionalized diaryl ether exhibited the most favorable thermodynamics for U binding and was chosen as the model system to study. Three polymer formulations were prepared with different monomer:cross-linker ratios (BAP 1-3). For all three formulations, FTIR analysis of dry material showed complete or nearly complete conversion of the nitrile functionality due to the greatly diminished C≡N stretch at 2250 cm^{-1}.

Large scale adsorption experiments were performed in an effort to accurately determine uranium adsorption capacity over time by ensuring an excess of U is present at all time points. Experiments were performed using 2 mg of BAP material in 370 mL seawater simulant spiked with 8 ppm U and 4.5 ppm V. A simultaneous control experiment without polymer was performed under identical conditions to confirm adsorption was attributable to binding by the hydrogel, rather than precipitation or physisorption onto the vessel walls. Aliquots were taken in triplicate at various time points and centrifuged at 13,000 rpm for 30 minutes. The supernatant

was then analyzed by ICP-MS and compared to the control to determine U sorption capacity. The results are shown in Figure 7.

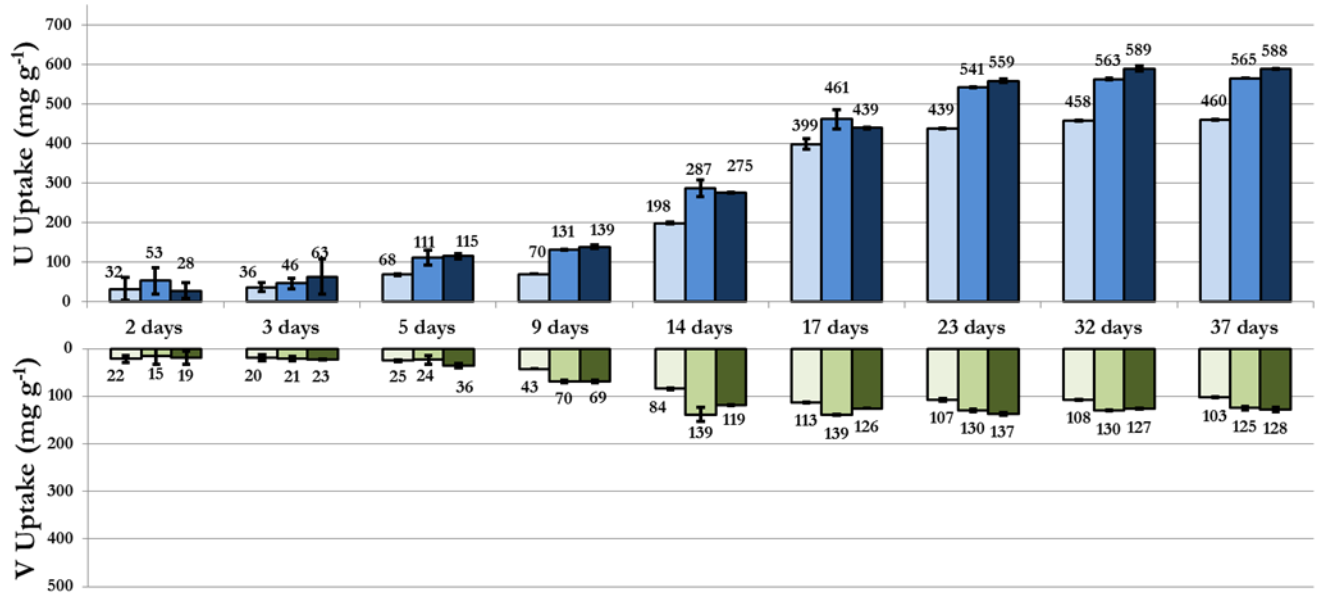

Figure 7: U and vanadium uptake trials over time. Top: U uptake of BAP materials in ~8 ppm U seawater simulant. Bottom: Vanadium uptake of hydrogel materials in 4.5 ppm V seawater simulant. Darkest bar is BAP 3, middle bar is BAP 2, lightest bar is BAP 1.

After 37 days, the BAP materials were able to adsorb nearly 600 mg U g^{-1} polymer in 8 ppm U spiked seawater simulant. Concomitant vanadium uptake in 4.5 ppm V spiked seawater simulant was nearly 5 times lower by weight—128 mg V g^{-1} polymer. Historically, non-specific adsorption of vanadium, zinc, and iron has greatly hindered the uranium sorption capacity of state of the art U sorption materials. Previous sorbents have exhibited high vanadium uptake exceeding 3:1 w/w, supposedly due to the formation of cyclic imidedioxime binding sites that possess stronger affinity for vanadium over uranium. The BAP system is unable to form cyclic imidedioxime sites and the only binding capable of occurring is through the amidoxime functionality. As a result, selectivity for U is dramatically improved and a 1:1 molar uptake of U:V is achieved.

Raman spectroscopy was used to investigate the nature of the observed uranyl binding and confirm that strong binding is responsible for the realized selectivity. The uranyl contacted BAP hydrogel exhibits a ν_1 stretch of 744.6 cm^{-1} in comparison to the state of the art amidoxime functionalized polymer fiber after laboratory adsorption tests which exhibits a ν_1 of 802.8 cm^{-1} (Figure 8). The shift towards lower wavenumber indicates pronounced electron donation from the amidoxime functionalities to the uranyl center suggestive of strong uranyl binding in the hydrogel materials being studied. This work has been submitted for publication and is currently under revision.

Summary

Over the course of this grant, our group has made several significant discoveries which have great potential in advancing the development of technologies to extract uranium from seawater. A series of uranyl-contacted amidoxime-functionalized polymer fibers were analyzed by EXAFS to investigate the amidoxime bonding motif. In seawater simulant, the local atomic coordination environment was most consistent with chelation by 2-3 amidoxime functionalities, with computational results indicating two cooperating ligands to be most defensible thermodynamically.

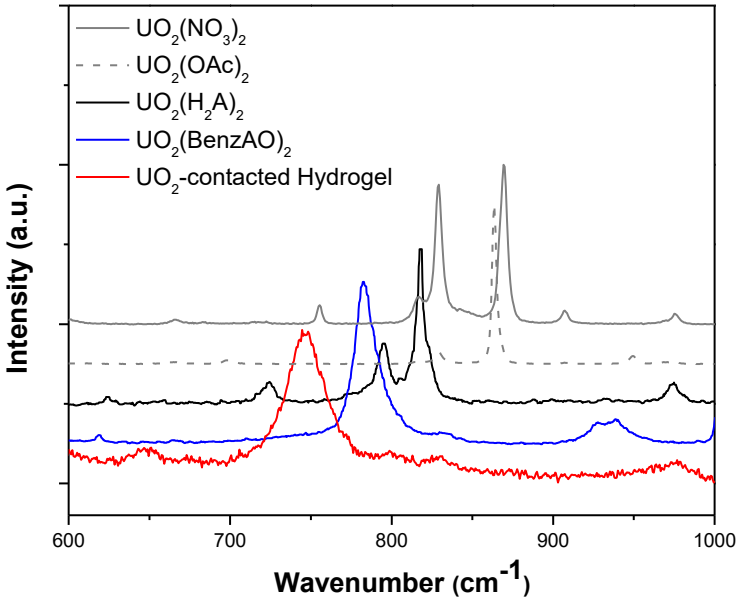

Figure 8 Raman spectra of various uranyl species.

Interested by the cooperative binding observed in the polymer samples, a new material was synthesized that shows great potential in aqueous uranium sequestration for applications to the nuclear fuel cycle. Using density-functional theory as a high throughput tool to quickly and efficiently screen several ligand types, a bifunctional chelator based on a flexible diaryl-ether framework, was chosen as the model system to study. Although uranyl binding did not occur through cooperative interactions by adjacent functionalities as expected, uranium sorption was nevertheless achieved. Indeed, uranium saturation capacity of 553 mg U g^{-1} sorbent was observed in seawater simulant, which surpasses the current state of the art materials by several-fold. EXAFS analysis suggests the formation of a coordination polymer with the carboxylate and amidoxime moieties bonding distinct uranyl groups. This ligand may have direct application for deployment in liquid-liquid extractions.

Encouraged by these results, Bis-amidoxime functionalized diaryl ethers were vinylated and co-polymerized with various ratios of hydrophilic crosslinker N,N'-methylenebisacrylamide to yield three batches of polymer materials with ligand loading upwards of 2 mmol g^{-1} as determined via FTIR. The polymer materials were investigated for uranium and vanadium adsorption over 37 days in pH 8.3 solution. Uranium sorption follows a sigmoidal shape with slow U uptake within 7 days, a rapid increase within 14 days, and a leveling off after 32 days. Vanadium (present as VO_4^{3-}) uptake follows a similar form. We observed a maximum U capacity of 588 mg U g^{-1} polymer and a maximum V capacity of 128 mg V g^{-1} polymer after 37 days—a near 5:1 w/w selectivity.

Raman spectroscopy, performed on the solid hydrogel sample along with several crystalline standards was used to probe further the nature of this selectivity. Compared with

crystalline uranium salts, the U saturated polymer exhibits a dramatically red-shifted ν_1 stretching frequency of 745 cm^{-1}. This ν_1 value is among the lowest in the literature and suggests pronounced electron donation to the uranium center.

(1) Oak Ridge National Lab. DOE Office of Nuclear Energy Fuel Resources Uranium from Seawater Program - Program Review Document. **2013**.
(2) Gupta, C. K.; Singh, H. *Uranium Resource Processing: Secondary Resources*; 2003.
(3) Witte, E. G.; Schwochau, K. S.; Henkel, G.; Krebs, B. Uranyl Complexes of Acetamidoxime and Benzamidoxime. Preparation, Characterization, and Crystal Structure. *Inorganica Chim. Acta* **1984**, *94* (6), 323–331.
(4) Kim, J.; Tsouris, C.; Oyola, Y.; Janke, C. J.; Mayes, R. T.; Dai, S.; Gill, G.; Kuo, L. J.; Wood, J.; Choe, K. Y.; Schneider, E.; Lindner, H. Uptake of Uranium from Seawater by Amidoxime-Based Polymeric Adsorbent: Field Experiments, Modeling, and Updated Economic Assessment. *Ind. Eng. Chem. Res.* **2014**, *53* (14), 6076–6083.
(5) Lindner, H.; Schneider, E. Review of Cost Estimates for Uranium Recovery from Seawater. *Energy Econ.* **2015**, *49*, 9–22.
(6) Tamada, M. Technology of Uranium Recovery from Seawater. *J. Jpn. Inst. Energy* **2009**, *88*, 249–253.
(7) Schenk, H. J.; Astheimer, L.; Witte, E. G.; Schwochau, K. Development of Sorbers for the Recovery of Uranium from Seawater. 1. Assessment of Key Parameters and Screening Studies of Sorber Materials. *Sep. Sci. Technol.* **1982**, *17* (11), 1293–1308.
(8) Kang, S. O.; Vukovic, S.; Custelcean, R.; Hay, B. P. Cyclic Imide Dioximes: Formation and Hydrolytic Stability. *Ind. Eng. Chem. Res.* **2012**, *51* (19), 6619–6624.
(9) Vukovic, S.; Watson, L. A.; Kang, S. O.; Custelcean, R.; Hay, B. P. How Amidoximate Binds the Uranyl Cation. *Inorg. Chem.* **2012**, *51* (6), 3855–3859.
(10) Chilou, V.; Gouzerh, P.; Jeannin, Y.; Robert, F. Synthesis and X-Ray Structures of molybdenum(VI)complexes with Benzamide Oximes. A Rare Linear Tetramolybdenum Compound [Mo4O11{p-TolC(NH2)NHO}2{p-TolC(NH)NHO}{p-TolC(NH)NO}]-. *J. Chem. Soc. Chem. Commun.* **1989**, *6* (76), 76.
(11) Kropf, A. J.; Katsoudas, J.; Chattopadhyay, S.; Shibata, T.; Lang, E. A.; Zyryanov, V. N.; Ravel, B.; McIvor, K.; Kemner, K. M.; Scheckel, K. G.; Bare, S. R.; Terry, J.; Kelly, S. D.; Bunker, B. A.; Segre, C. U. The New MRCAT (Sector 10) Bending Magnet Beamline at the Advanced Photon Source. *AIP Conf. Proc.* **2010**, *1234* (Sector 10), 299–302.
(12) Abney, C. W.; Mayes, R. T.; Piechowicz, M.; Lin, Z.; Bryantsev, V. S.; Veith, G. M.; Dai, S.; Lin, W. XAFS Investigation of Polyamidoxime-Bound Uranyl Contests the Paradigm from Small Molecule Studies. *Energy Environ. Sci.* **2016**, *9* (2), 448–453.
(13) Abney, C. W.; Das, S.; Mayes, R. T.; Kuo, L.-J.; Wood, J.; Gill, G.; Piechowicz, M.; Lin, Z.; Lin, W.; Dai, S. A Report on Emergent Uranyl Binding Phenomena by an Amidoxime Phosphonic Acid Co-Polymer. *Phys. Chem. Chem. Phys.* **2016**, *18* (34), 23462–23468.
(14) Piechowicz, M.; Abney, C. W.; Zhou, X.; Thacker, N. C.; Li, Z.; Lin, W. Design, Synthesis, and Characterization of a Bifunctional Chelator with Ultrahigh Capacity for Uranium Uptake from Seawater Simulant. *Ind. Eng. Chem. Res.* **2016**, *55* (15), 4170–4178.